Sustainable Civil Building Management and Engineering Journal Vol: 2, No 2, 2025, Page: 1-15

Analysis of the Effect of Boro River Backwater as an Impact of Flood Inundation in Sewu Urban Village, Surakarta City

Syakira Madina Noor Amina*, Rr. Rintis Hadiani, Solichin

Civil Engineering Study Program, Faculty of Engineering, Universitas Sebelas Maret

DOI:
https://doi.org/10.47134/scbmej.v2i2.3759
*Correspondence: Syakira Madina Noor Amina
Email: syakiraamina@gmail.com

Received: 21-02-2025
Accepted: 21-03-2025
Published: 21-04-2025

Abstract: Backwater is a condition where the flow of river water is obstructed, causing the water level to rise and overflow into the surrounding area. The backwater phenomenon is the main cause of flood inundation in Sewu Village. The confluence of two rivers, namely the main Bengawan Solo River and the Boro River, causes the flow of water from the Boro River to be obstructed due to the higher elevation of the River in the Bengawan Solo River. Therefore, this study aims to analyze the effect of the Boro River backwater on flood inundation in Sewu Village with a 20-year (Q_{20}), 25-year (Q_{25}), and 50-year (Q_{50}) return period flood discharge using the Soil Conservation Service synthetic unit hydrograph method with HEC-HMS software. This research uses hydraulic simulation by simulating river flow to find out the location of backwater that causes runoff. The results showed that the 20-year return period flood discharge (Q_{20}) of 14.7 m^3/s, 25-year return period (Q_{25}) of 15.2 m^3/s, and 50-year return period (Q_{50}) of 16.6 m^3/s significantly affected the water level in Boro River, which resulted in an increase in the flood inundation area in Sewu Village. Hydraulic simulations revealed that the critical point of backwater in Boro River affects the maximum water depth of the river, such as the 20-year return period (Q_{20}) has an increase difference of 0.32 meters, the 25-year return period (Q_{25}) of 0.25 meters, and the 50-year return period (Q_{50}) of 0.68 meters.

Keywords: Backwater, Flood Inundation, HEC-HMS, HEC-RAS

Introduction

Sewu Village is one of the areas in Jebres Sub-district, Surakarta City, that is directly adjacent to the Bengawan Solo River, Boro River, and Pepe River, making this area vulnerable to overflowing water due to high rainfall and the phenomenon of backwater that results in flood inundation.

Backwater is a phenomenon when water flow in a river is obstructed, causing the water level to rise and overflow into the surrounding area. This phenomenon occurs due to the confluence of two rivers where one of the rivers has a higher water level. The occurrence of backwater is an interaction effect between flood waves in the main river and tributaries that can extend up to several kilometers upstream of the tributary, especially if the river has a gentle slope (Dyhouse, 1985). This can certainly cause flood inundation, especially in low-lying areas. Research on backwater in lowland rivers shows that backwater is usually reciprocal and determined by discharge (Chen et al., 2023).

When tributaries are exposed to backwater from the mainstream, there is a rise in water level and a decrease in velocity. As a result of high rainfall, it causes inundation. Given Sewu Village's proximity to the Bengawan Solo, Pepe, and Boro Rivers, it is necessary to study the impact of inundation in the Boro River due to flooding. To be able to predict and anticipate these events more accurately, historical data on river flow discharge up to the last year is needed (Rahman et al., 2018) . However, no measured data results with discharge return times up to the last year. Therefore, in this study, an analysis of inundation events in Boro River in Sewu Village was conducted with 20-year (Q_{20}), 25-year (Q_{25}), and 50-year (Q_{50}) return time flood discharge with rainfall data from 2004 - 2023.

In conducting research, hydraulic modeling can accurately predict inundation patterns (H. U. A. Khan et al., 2017). Therefore, this study uses hydraulic models in the form of rational methods or empirical methods, such as the SCS Synthetic Unit Hydrograph (HSS) integrated with geospatial data to obtain a return time plan discharge with more accurate results. Hydraulic modeling is the main component that can predict inundation height. Accurate and reliable predictions of inundation height can help prevent potential flood inundation (Bessar et al., 2020) . To model the potential flood inundation that can occur, HEC-RAS software is used in combination with extensions to ArcGIS software. The use of HEC-RAS and ArcGIS software has been shown to have a strong correlation in evaluating inundation risk and reliably forecasting future floods (S. Khan et al., 2022).

This research was conducted to determine the occurrence of Boro River backwater in Sewu Village without taking into account the existence of floodgates. The occurrence of backwater in Sewu Village is due to the increase in water discharge in the Bengawan Solo River, which results in backwater in the Boro River. When the water discharge of the Bengawan Solo River increases, the water level also increases, causing the flow of water from the Boro River to be blocked and return upstream. This condition caused the water level in Boro River to increase significantly, exceeding the capacity of the channel and causing overflows that inundated Sewu Village.

Methodology

This research uses a quantitative descriptive method approach. The data used includes maximum rainfall from 2004 to 2023 from the Mojolaban, Grogol, and Ngemplak rain stations obtained from the Bengawan Solo River Basin Center (BBWS). In addition, administrative map data of Sewu village and DEM map of Jebres sub-district obtained from the Geospatial Information Agency (BIG) were also used for processing. The data was then analyzed to determine the 20-year (Q_{20}), 25-year (Q_{25}), and 50-year (Q_{50}) return period flood discharge. The analysis used to determine the most suitable rainfall distribution uses several methods, namely the Log Normal, Log Pearson Type III, Normal, and Gumbel methods. Distribution suitability tests were also conducted using the Smirnov-Kolmogorov and Chi-Square tests.

Repeat-time flood discharge was then conducted using the Soil Conservation Service synthetic unit hydrograph method with HEC-HMS software. The obtained return-time flood discharge is then used as input in hydraulic simulation with HEC-RAS software. Simulations were conducted to determine the point of backwater occurrence, maximum depth of water, and inundation area with the influence of backwater and without the influence of backwater. The simulation results are compared to determine how much influence backwater has on the maximum depth of water and the inundation area.

Result and Discussion

This research is located in Sewu Village, Jebres Sub-district, Surakarta City. Sewu Village is traversed by the Boro River and Bengawan Solo River.

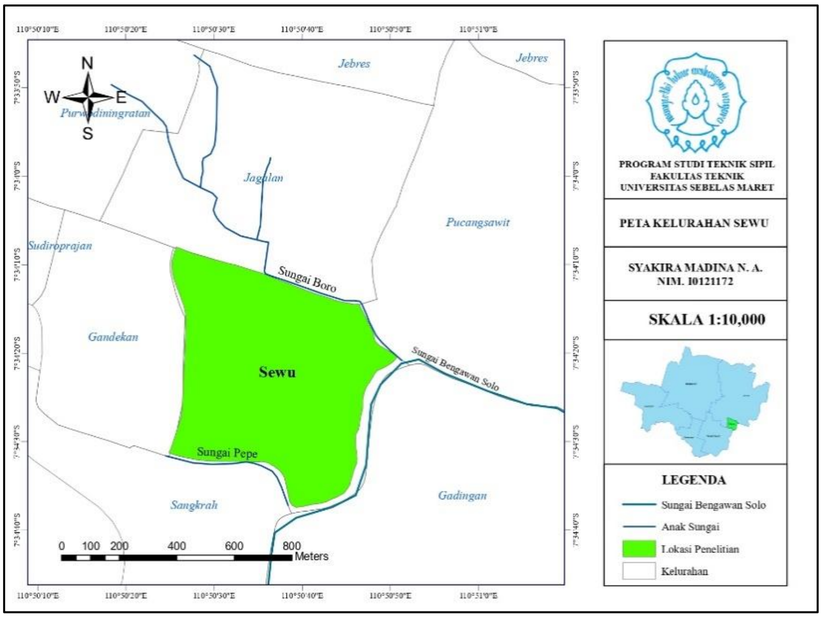

Figure 1. Sewu Village
Source: Sewu Village Picture

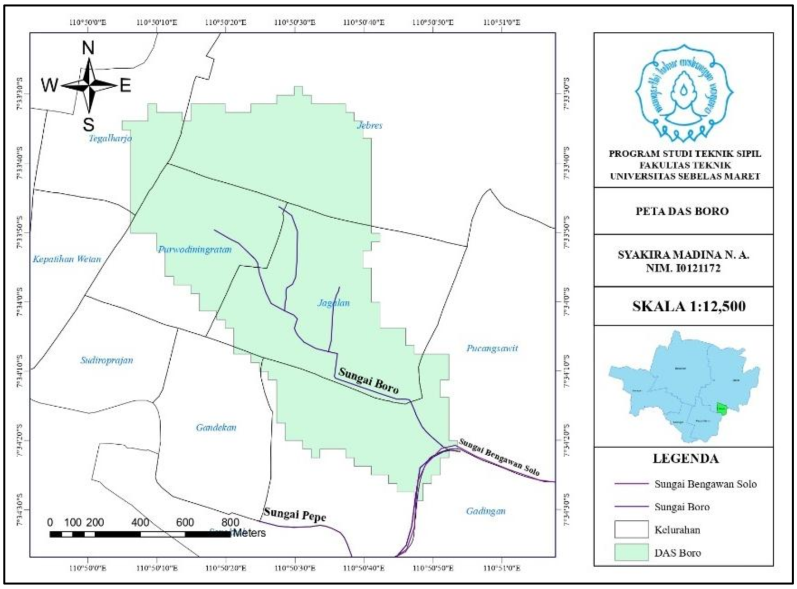

Figure 2. Boro River Watershed Map
Source: Analysis Results, 2024

In this study, the river whose flow discharge is calculated is Boro River. From the Boro watershed analysis results, an area of 1.42 km² was obtained with the Thiessen coefficient of the influence of Mojolaban and Grogol rain stations presented in **Table 1** below.

Table 1. Thiessen Coeffiesien

No	Rain Station	Area (km²)	Thiessen Coeffisien (Ci)	(%)
1	Mojolaban	0.6885	0.4855	48.5461
2	Grogol	0.7297	0.5145	51.4539
Total Watershed Area		1.4182	1	100

The calculation of maximum daily rainfall from the rain station adjacent to the Boro watershed is then multiplied by the value of the Thiessen coefficient. **Table 2** presents the recapitulation results of maximum daily rainfall with Thiessen influence.

Table 2. Recapitulation of Maximum Daily Rainfall with Thiessen Effect

No.	Year	Month	Mojolaban Rain Station Ci = 0.4855		Grogol Rain Station Ci = 0.5145		RH (mm)	RH Max (mm)
			Xi	Xi.Ci	Xi	Xi.Ci		
1	2004	1-15 Januari	114.00	55.34	62.00	31.90	87.24	95.64
		16-31 Januari	126.00	61.17	67.00	34.47	95.64	
2	2005	1-15 Maret	110.00	53.40	31.00	15.95	69.35	53.40
		1-15 Juli	85.00	41.26	23.00	11.83	53.10	
3	2006	1-15 Januari	60.00	29.13	0.00	0.00	29.13	47.58
		16-31 Januari	98.00	47.58	0.00	0.00	47.58	
4	2007	1-15 Februari	100.00	48.55	83.21	42.81	91.36	110.40
		16-30 April	118.00	57.28	103.22	53.11	110.40	
No.	Year	Month	Mojolaban Rain Station Ci = 0.4855		Grogol Rain Station Ci = 0.5145		RH (mm)	RH Max (mm)
			Xi	Xi.Ci	Xi	Xi.Ci		
5	2008	1-15 Maret	137.00	66.51	59.00	30.36	96.87	87.60
		16-31 Maret	77.00	37.38	72.00	37.05	74.43	
6	2009	1-15 Januari	63.00	30.58	88.00	45.28	75.86	104.55
		16-31 Januari	138.00	66.99	73.00	37.56	104.55	
7	2010	1-15 November	104.00	50.49	109.00	56.08	106.57	102.97
		1-15 Februari	69.00	33.50	95.00	48.88	82.38	
8	2011	1-15 November	99.00	48.06	95.00	48.88	96.94	88.69
		1-15 Desember	83.00	40.29	85.00	43.74	84.03	
9	2012	1-15 Januari	121.00	58.74	104.00	53.51	112.25	112.25
		16-29 Februari	104.00	50.49	86.53	44.52	95.01	
10	2013	16-31 Mei	83.00	40.29	77.46	39.85	80.15	81.52
		16-31 Oktober	86.00	41.75	99.00	50.94	92.69	
11	2014	1-15 Januari	87.00	42.24	72.39	37.25	79.48	79.48
		16-31 Desember	84.00	40.78	70.00	36.02	76.80	
12	2015	1-15 April	54.00	26.21	52.49	27.01	53.22	81.09
		16-31 Maret	78.00	37.87	84.00	43.22	81.09	
13	2016	1-15 November	105.00	50.97	87.70	45.13	96.10	96.10

		16-30 Juni	104.00	50.49	86.53	44.52	95.01	
14	2017	16-30 April	128.00	62.14	52.00	26.76	88.90	98.49
		16-30 November	154.00	74.76	98.00	50.42	125.19	
15	2018	1-15 Februari	98.00	47.58	90.00	46.31	93.88	85.15
		1-15 November	78.00	37.87	73.00	37.56	75.43	
16	2019	16-31 Januari	98.00	47.58	53.26	27.40	74.98	78.96
		1-15 April	83.00	40.29	68.00	34.99	75.28	
17	2020	1-15 Maret	97.00	47.09	81.46	41.91	89.00	95.58
		16-30 November	128.00	62.14	69.00	35.50	97.64	
18	2021	16-31 Agustus	127.00	61.65	95.53	49.16	110.81	104.01
		1-15 November	127.00	61.65	90.64	46.64	108.29	
19	2022	16-30 April	65.58	31.84	75.00	38.59	70.43	82.02
		1-15 Mei	68.64	33.32	95.00	48.88	82.20	
20	2023	1-15 Maret	157.00	76.22	133.94	68.92	145.13	144.47
		1-15 Mei	94.00	45.63	73.76	37.95	83.58	

The results of the rainfall distribution analysis with the four distribution methods are presented in **Table 3**.

Table 3. Recapitulation of Rainfall Distribution Analysis Results

Period (year)	Log-Normal	Log Pearson III	Normal	Gumbel
20	133.10	119.69	125.57	139.32
25	135.35	125.08	126.99	143.78
50	147.15	129.24	134.09	157.53

From the results of the distribution analysis, the next step is to test the suitability to choose the rainfall distribution method that will be used. The suitability of the distribution is tested using the dispersion test, Chi-Square test, and Smirnov-Kolmogorov test. The results of the dispersion test calculations are then compared to determine the most suitable distribution type presented in **Table 4**.

Table 4. Dispersion Test Calculation Results

Type of Distributions	Terms	Calculation Result	Description
Log-Normal	$Cs \approx 3\ Cv + Cv^2 = 3$	$Cs = -0.9515$	Not eligible
	$Ck \approx Cv^3 + 6Cv^6 + 15\ Cv^4 + 16\ Cv^2 + 3$	$Ck = 5.4766$	
	$Cv = 0.0545$	$Cv = 0.0545$	
Log Pearson III	$Cs \neq 0$	$Cs = -0.9515$	Not eligible
	$Cs = 5.672$	$Ck = 5.4766$	
	$Cs = 0.042$	$Cv = 0.0545$	
Normal	$Cs \approx 0$	$Cs = 0.1526$	Not eligible
	$Ck = 3$	$Ck = 5.2369$	
Gumbel	$Cs \leq 1.1396$	$Cs = -0.9515$	Qualified
	$Ck \leq 5.4002$	$Ck = 5.2369$	

From the test results, the Gumbel distribution method was selected. Furthermore, Chi-Square and Smirnov-Kolmogorov tests were conducted, and the following results were obtained.

- Chi-Kuadrat (terms, x^2 result < x^2 Cr)
  x^2 result = 5.7500
  x^2 Cr = 7.8150
  so, 5.7500 < 7.8150 (Gumbel method qualified)

- Smirnov-Kolmogorov (terms, Dmax < Do)
  Dmax = 0.1816
  Do = 0.2941
  so, 0.1816 < 0.2941 (Gumbel method qualified)

Thus, from the results of the three stages of testing, the Gumbel method. Then, the rainfall plan based on the Gumbel method with a return time is obtained as in **Table 5**.

Table 5. Rainfall Recurrence Period with Gumbel Method

Return Period (Year)	Rainfall (mm)
20	139.32
25	143.78
50	157.53

The time series flood discharge is analyzed using the Soil Conservation Service synthetic unit hydrograph method with HEC-HMS software. This software will model and simulate the relationship between rainfall and surface runoff. The running results obtained are hydrographs for 20-year (Q_{20}), 25-year (Q_{25}), and 50-year (Q_{50}) return period discharge.

Table 6. Hydrological Characteristics of Boro Watershed

Subbasin	Longest Flow Path (km)	Basin Slope (m/m)	Longest Flow Path (m)	Basin Slope (%)	tc (min)	tc (hours)	Lagtime (hours)	S	Ia (mm)
Boro	1.56	0.0051	1560.00	0.51	143.46	2.39	1.43	47.86	9.57

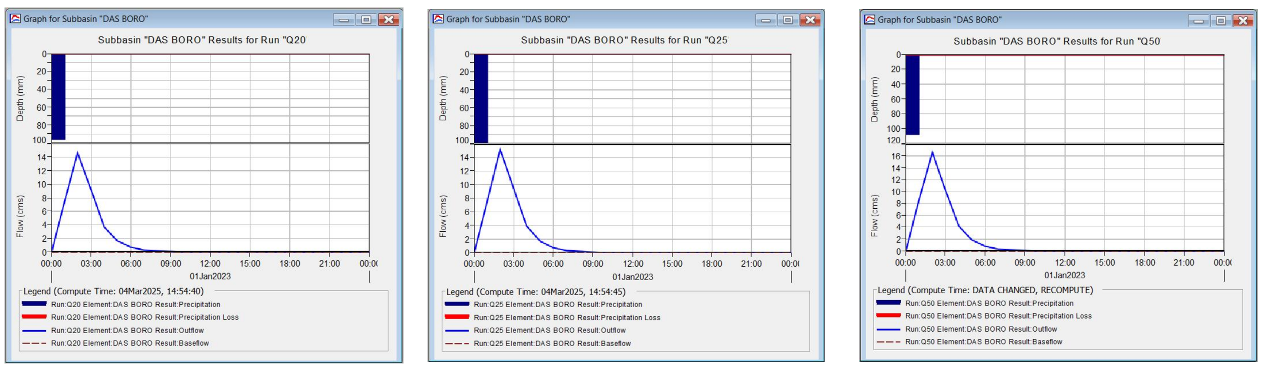

20 Years 25 Year 50 Years

Figure 3. Hydrograph of Return Period Flood Discharge of Boro Watershed in HEC-HMS
Source: Image of running HEC-HMS software

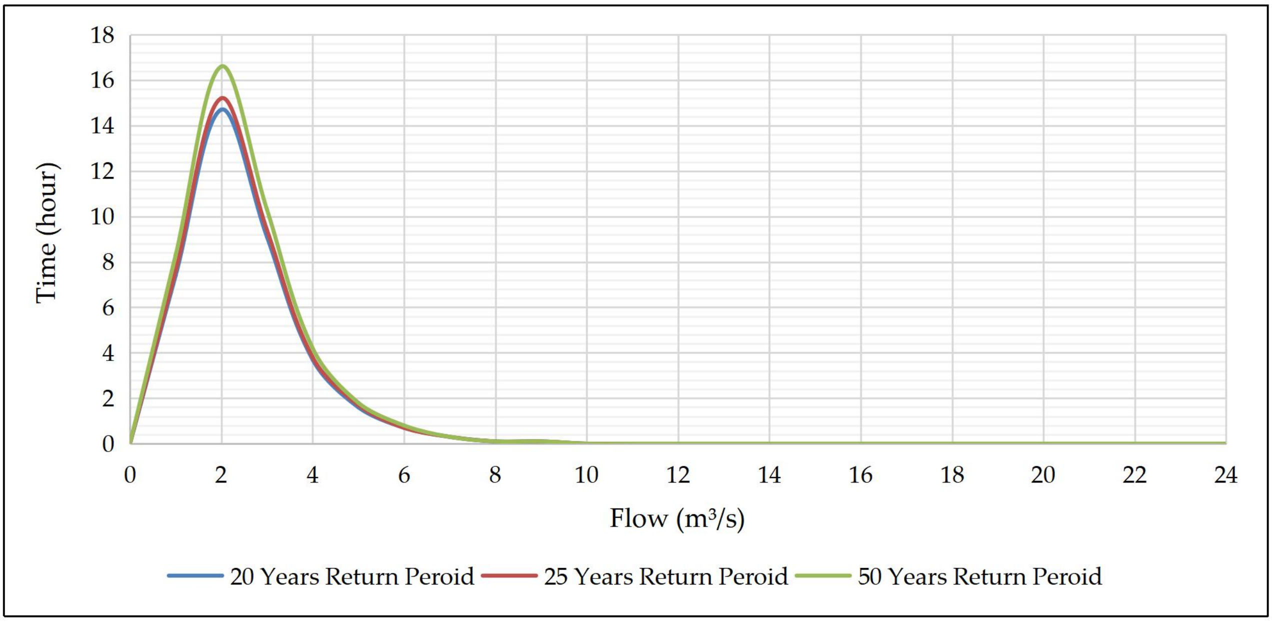

Figure 4. Hydrograph of Return Period Flood Discharge of Boro Watershed
Source: Analysis Results, 2024

To determine the location of the backwater and the comparison of the increase in the inundation area due to the influence of backwater and without the influence of backwater, HEC-RAS software is used. This software is used to perform hydraulic analysis. In this study, 2D non-fixed flow cross-sectional modeling is used. This analysis is carried out with 20-year (Q_{20}), 25-year (Q_{25}), and 50-year (Q_{50}) return period flood discharges. The location of the Boro River backwater review point is presented in Figure 5.

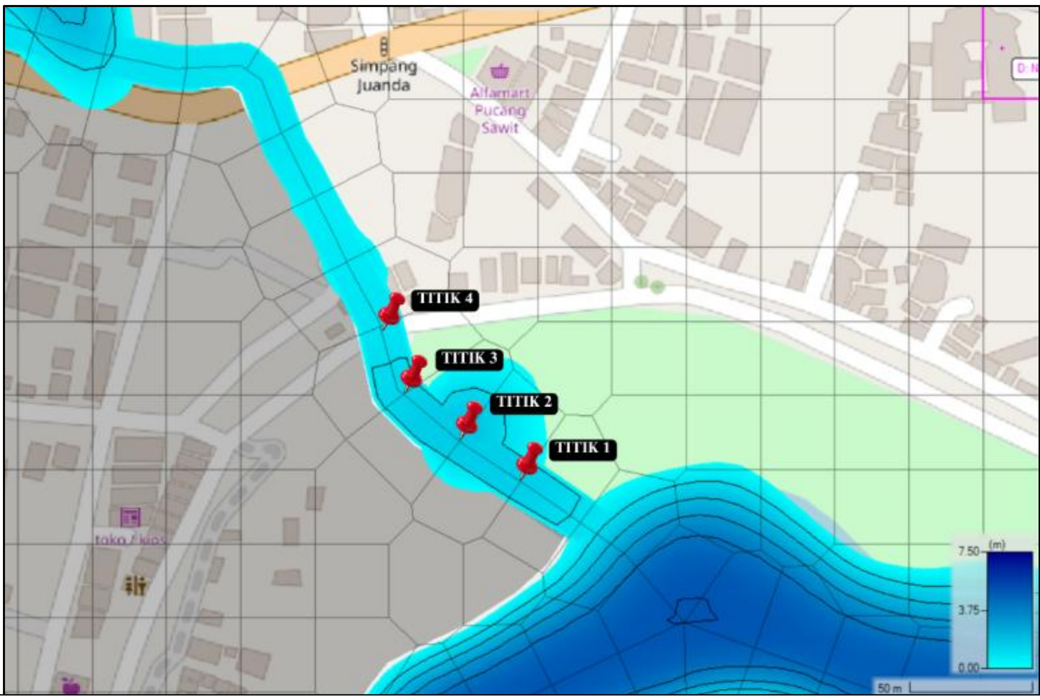

20 Years

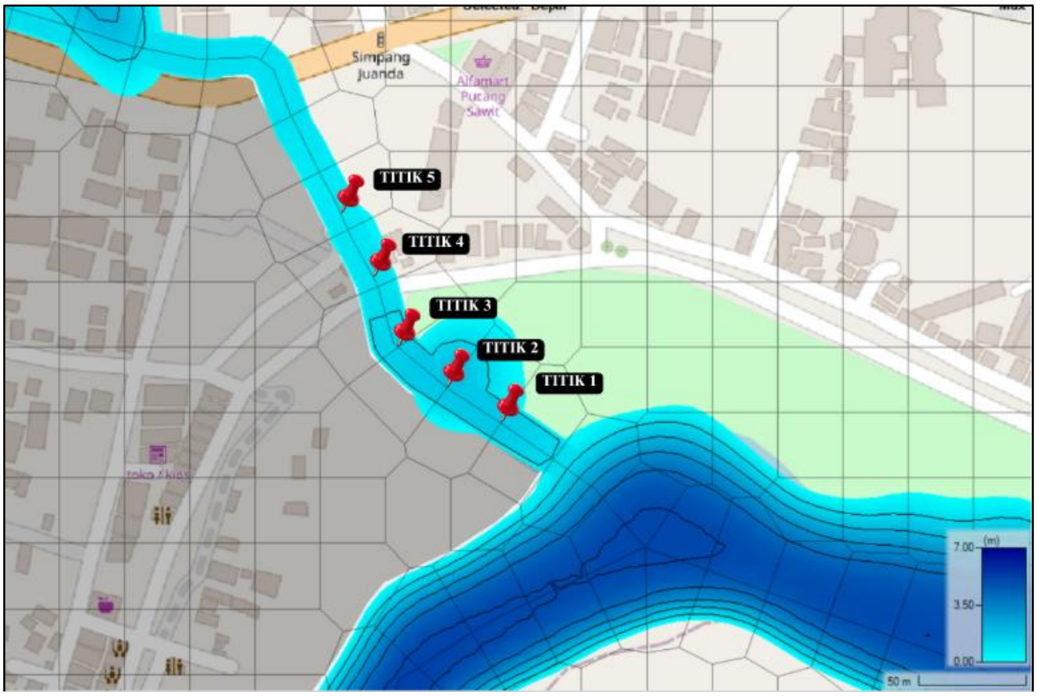

25 Years

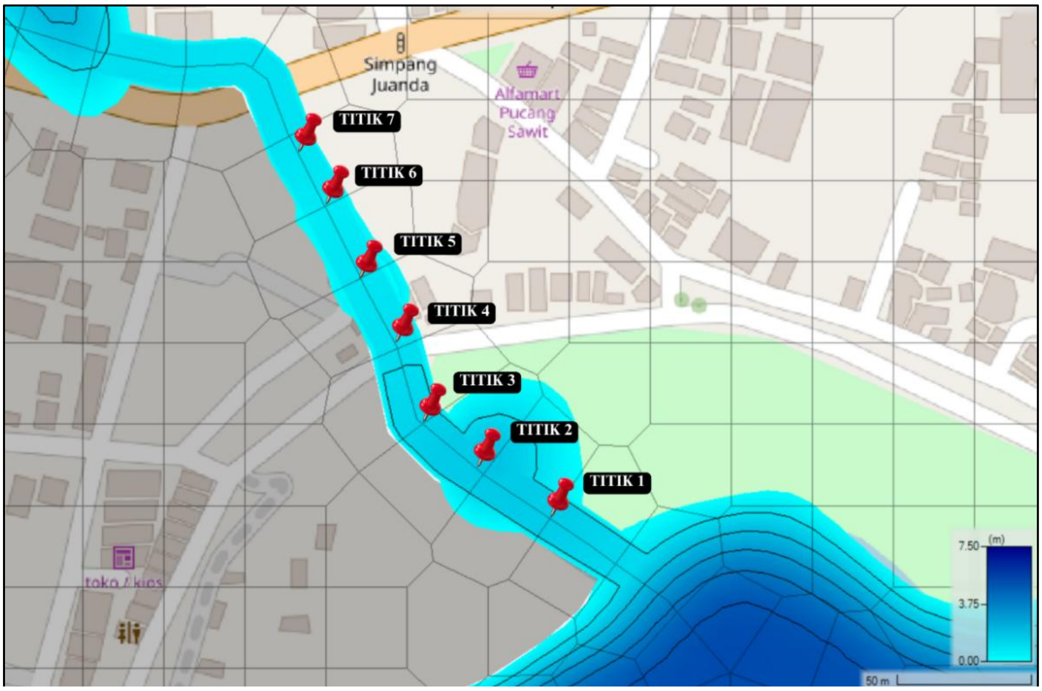

50 Years

Figure 5. Location Point of Boro River Backwater Occurrence
Source: Image of Location Point in HEC-RAS software

The water depth for each point with 20-year (Q_{20}), 25-year (Q_{25}), and 50-year (Q_{50}) return period flood discharge due to the influence of backwater and without the influence of backwater has a difference. The effect of backwater causes the water depth to increase significantly along with the increase in distance or length of flow. The distance or length of water flow affected by backwater in the Boro River for Q_{20} can be seen in **Table 7**. Meanwhile, the results of water depth for the 20-year return period flood discharge (Q_{20}) can be seen in **Figure 6**.

Table 7. Backwater length of Boro River for Q20

Point Location			Distance (m)
0	-	Point 1	29.4
Point 1	-	Point 2	29.4
Point 2	-	Point 3	29.4
Point 3	-	Point 4	28.3
Backwater Length			116.5

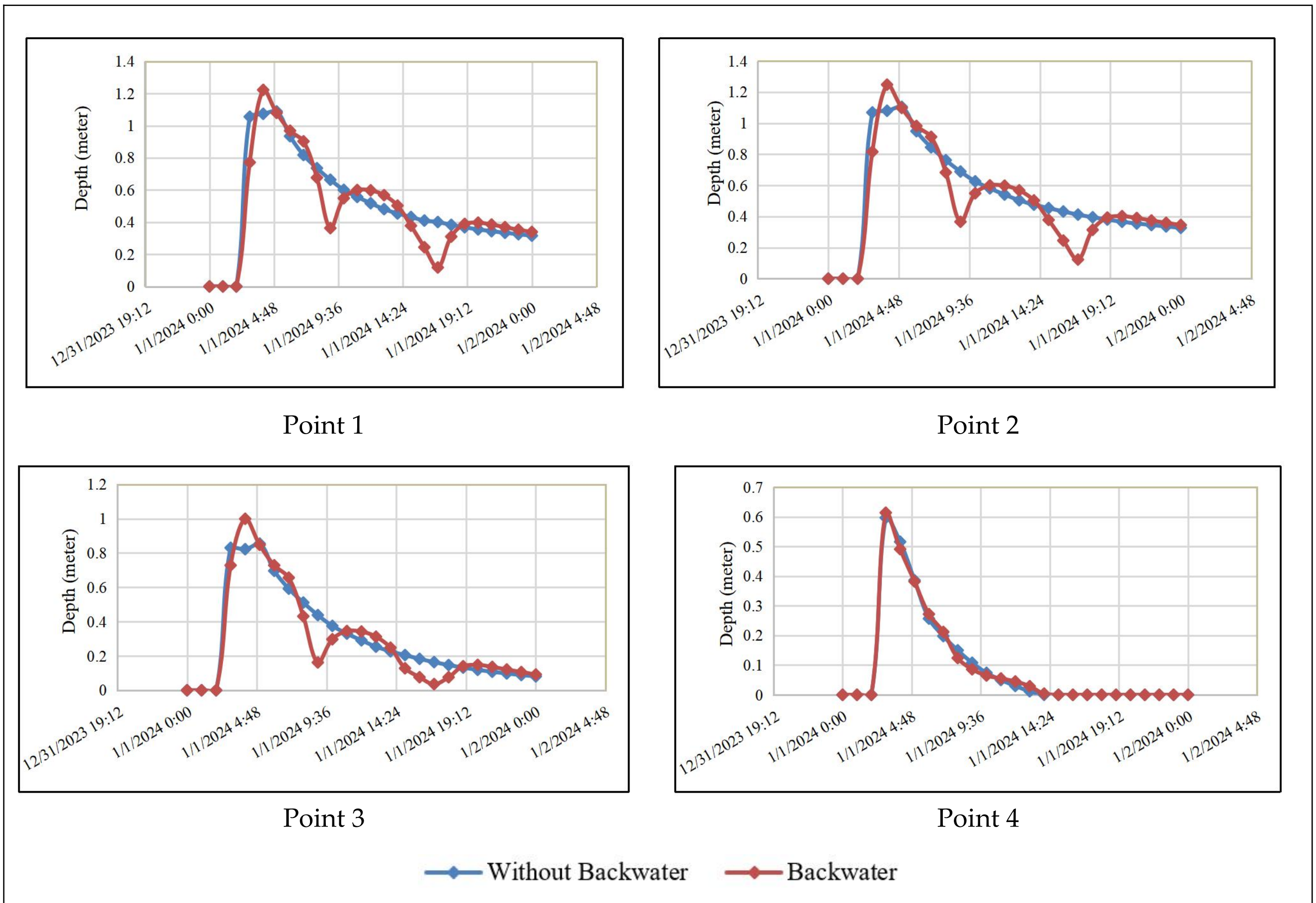

Figure 6. Q_{20} Water Depth Chart
Source: Analysis Results, 2024

From the results of the graph above, the water depth at each point for Q_{20} with the influence of backwater increases until it has the same depth as without the influence of backwater. This indicates that the location of the backwater is at point 1 to point 4, where point 2 has a maximum water depth of 1.248 m on 1 January at 04.00 WIB. After reaching the peak point, at point 2 on 1 January at 09.00 WIB, there was a significant decrease in water depth with a difference in water depth due to the influence of backwater of 0.366 m and without the influence of backwater amounting to 0.689 m. The length of water flow affected by the backwater of the Boro River for Q_{25} can be seen in **Table 8**. Meanwhile, the results of the water depth for the 25-year return period flood discharge (Q_{25}) can be seen in **Figure 7**.

Table 8. Backwater length of Boro River for Q_{25}

Point Location			Distance (m)
0	-	Point 1	29.6
Point 1	-	Point 2	29.6
Point 2	-	Point 3	29.6
Point 3	-	Point 4	34.6
Point 4	-	Point 5	37.1
Backwater Length			160.5

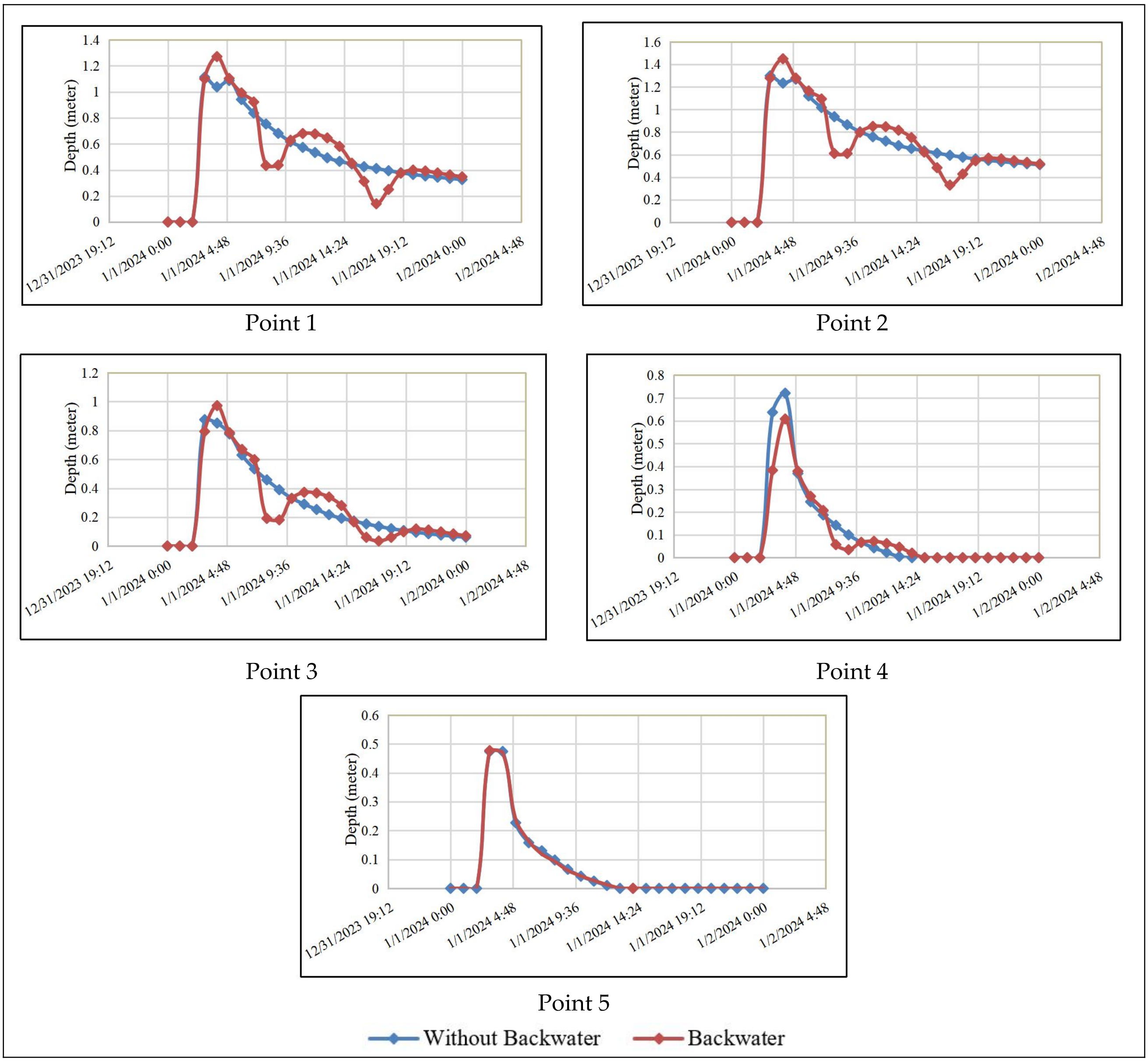

Figure 7. Q_{25} Water Depth Chart
Source: Analysis Results, 2024

From the results of the graph above, the water depth at each point for Q_{25} with the influence of backwater increases until it has the same depth as without the influence of backwater. This indicates that the location of the backwater is at point 1 to point 5, where point 2 has a maximum water depth of 1.449 m on 1 January at 04.00 WIB. After reaching the peak point, at point 2 on 1 January at 09.00 WIB, there was a significant decrease in water depth with a difference in water depth due to the influence of backwater of 0.610 m and without the influence of backwater or normal conditions of 0.865 m. The length of water flow affected by the backwater of the Boro River for Q_{50} can be seen in **Table 9**. Meanwhile, the results of the water depth for the 50-year return period flood discharge (Q_{50}) can be seen in **Figure 8**.

Table 9. Backwater length of Boro River for Q_{50}

Point Location			Distance (m)
0	-	Point 1	29.4
Point 1	-	Point 2	29.4
Point 2	-	Point 3	29.4
Point 3	-	Point 4	29.4
Point 4	-	Point 5	29.4
Point 5	-	Point 6	29.4
Point 6	-	Point 7	23.8
Backwater Length			200.2

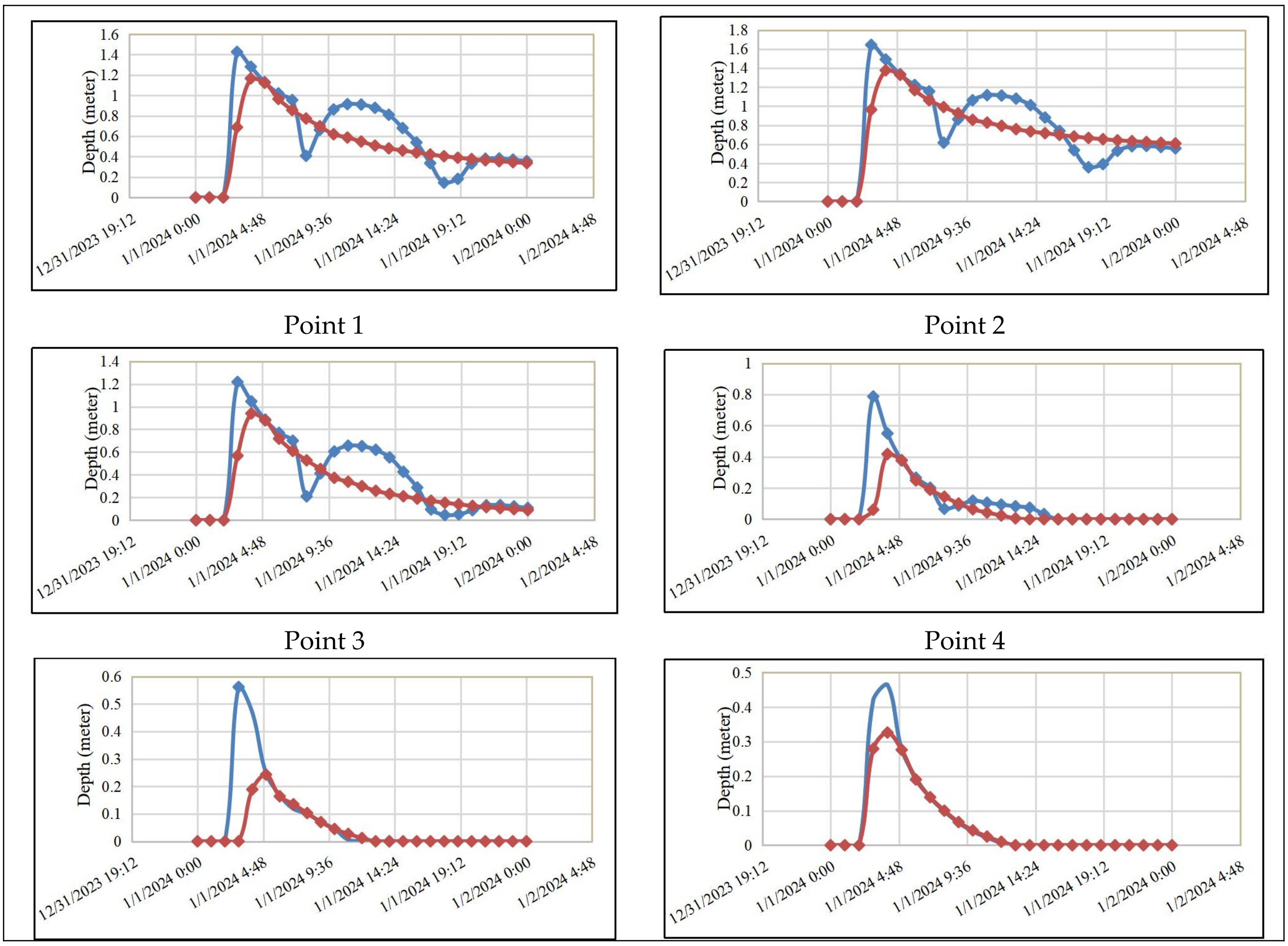

Point 5 Point 6

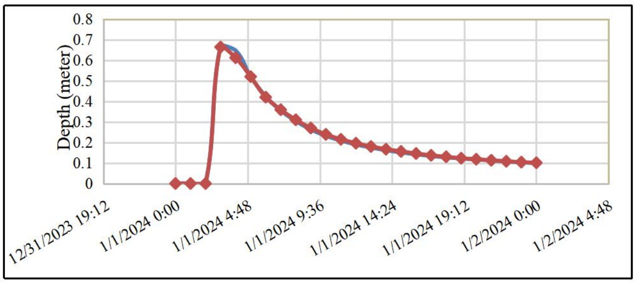

Point 7

Without Backwater Backwater

Figure 8. Q_{50} Water Depth Chart
Source: Analysis Results, 2024

From the results of the graph above, the water depth at each point for Q_{50} with the influence of backwater increases until it has the same depth as without the influence of backwater. This indicates that the location of the backwater is at point 1 to point 7, where point 2 has a maximum water depth of 1.644 m on 1 January at 03.00 WIB. After reaching the peak point, at point 2 on 1 January at 08.00 WIB, there was a significant decrease in water depth with a difference in water depth due to backwater of 0.617 m and without the influence of backwater of 0.991 m.

The depth due to the influence of backwater for Q_{20}, Q_{25}, and Q_{50} at the peak point is greater than without the influence of more stable backwater, this is because after reaching the peak point, the water decreases faster and fluctuates due to the influence of backwater which causes greater variation in changes in water depth. From the results of the graph above for Q_{20}, Q_{25}, and Q_{50}, it can also be seen that the further away from the meeting point of the Bengawan Solo River and the Boro River, in this case, point 6, the influence of backwater decreases and the depth of the water with the influence of backwater is closer to normal conditions (without the influence of backwater).

From the results of running HEC-RAS, the maximum flood inundation area for Q_{20}, Q_{25}, and Q_{50} in Sewu Village was obtained. The maximum flood inundation area due to the influence of backwater is greater than without the influence of backwater. The magnitude of the maximum flood inundation area due to the influence of backwater and without the influence of backwater for Q_{20}, Q_{25}, and Q_{50} can be seen in **Table 4.10**.

Table 10. Recapitulation of Maximum Flood Inundation Area

Return Period Flood Discharge	Area of Sewu Village (ha)	Maximum Flood Inundation Area with Backwater Influence (ha)	Maximum Flood Inundation Area without Backwater Influence (ha)
Q_{20}	44.6898	2,3667	1,2753
Q_{25}		2,4381	1,2906
Q_{50}		2,6295	1,3512

Based on the comparison table of the maximum flood inundation area for Q_{20}, Q_{25}, and Q_{50} in Sewu Village, there is a significant difference in results. The influence of backwater causes the flood inundation area to increase significantly when compared to normal conditions or without the influence of backwater. This happens because the river flow that slows down due to the influence of backwater causes water to overflow onto land, so the area inundated increases. The backwater phenomenon also occurs due to flow resistance downstream and causes the water level in the river to rise so that the existing flood discharge cannot flow normally. As a result, the volume of retained water increases and expands the area affected by flood inundation. The greater the flood discharge, in this case, Q_{20}, Q_{25}, and Q_{50}, the greater the influence of backwater on the inundation area formed.

Conclusion

Based on the results of the analysis of the influence of the backwater of the Boro River, it can be concluded that the maximum return time flood discharge with the soil in the Boro watershed for Q_{20} years of 14.7 m³/s, Q_{25} years 15.2 m³/s, and Q_{50} years 16.6 m³/s. Based on the results of the analysis with HEC-RAS, the flow length due to the influence of backwater for Q_{20} is 116.5 m. The critical point of backwater for Q_{20} is at point 2, which at that point has a maximum water depth of 1.248 m on January 1 at 04.00 WIB. After reaching the peak point, at point 2 on January 1 at 09.00 WIB, there was a significant decrease in water depth with a difference in water depth due to the influence of backwater of 0.366 m and without the influence of backwater or normal conditions of 0.689 m. The flow length due to the influence of backwater for Q_{25} is 160.5 m. The critical point of backwater for Q_{25} is also at point 2, which at that point has a maximum water depth of 1.449 m on January 1 at 04.00 WIB. After reaching the peak point, at point 2 on January 1 at 09.00 WIB, there was a significant decrease in water depth with a difference in water depth due to the influence of backwater of 0.610 m and without the influence of backwater or normal conditions of 0.865 m. The flow length due to the influence of backwater for Q_{25} is 200.2 m. The critical point of backwater for Q_{50} is at point 2, which at that point has a maximum water depth of 1.644 m on January 1 at 03.00 WIB. After reaching the peak point, at point 1 on January 1 at 08.00 WIB, there was a significant decrease in water depth with a difference in water depth due to the influence of backwater of 0.617 m and without the influence of backwater of 0.991 m. The effect of backwater will decrease with increasing time and distance from the confluence of the Bengawan Solo River with the Boro River. In addition, the influence of backwater will increase the flood inundation area significantly compared to without the influence of backwater, with the maximum flood inundation area for Q_{20} years of 2.3667 ha, Q_{25} years of 2.4381 ha, and Q_{50} years of 2.6295 ha which is greater than without the influence of backwater (normal conditions).

References

Alaghmand, S., Abdullah, R. bin, Abustan, I., & Vosoogh, B. (2010). GIS-based river flood hazard mapping in urban area (a case study in Kayu Ara river basin, Malaysia). *International Journal of Engineering and Technology*, *2*(6), 488–500.

Amin, M., Ir Ridwan, Ms., Ir Iskandar Zulkarnaen, M., & Jurusan Teknik Pertanian, Ms. (2018). Pengolahan Daerah Aliran Sungai. *LPPM UNILA Institutional Repository (LPPM-UNILA-IR)*, 9–92. http://repository.lppm.unila.ac.id/id/eprint/8538

Andina, E. (2019). The Analysis of Waste Sorting Behavior in Surabaya. *Jurnal Aspirasi*, *10*(2), 119–138. https://doi.org/10.22212/aspirasi.v10i2.1424

Anna, A. N., Cholil, M., Studi, P., Geografi, P., & Surakarta, U. M. (2015). Terhadap Banjir Luapan Sungai Bengawan Solo Hulu Tengah Pendahuluan The 2 nd University Research Coloquium 2015 ISSN 2407-9189. *The 2nd University Research Coloquium*.

Basuki, Winaesih. I., & Adhyani,. N. L. (2009). *Analisis Periode Ulang Hujan Maksimum Dengan Berbagai Metode* (J.Agromet).

Bessar, M. A., Matte, P., & Anctil, F. (2020). Uncertainty analysis of a 1D river hydraulic model with adaptive calibration. *Water (Switzerland)*, *12*(2). https://doi.org/10.3390/w12020561

Chen, Y., Xia, R., Jia, R., Hu, Q., Yang, Z., Wang, L., Zhang, K., Wang, Y., & Zhang, X. (2023). Flow backward alleviated the river algal blooms. *Water Research*, *245*(September), 120593. https://doi.org/10.1016/j.watres.2023.120593

Clark, M. J. (1998). Putting water in its place: a perspective in GIS in hydrology an water management. *Hydrological Processes*, *12*.

Dwiprayogo, B., Sisinggih, D., & Priyantoro, D. (2018). Studi Perencanaan Tanggul Banjir Di Sungai Bengawan Solo Pada Ruas Kota Surakarta, Jawa Tengah. *Jurnal Pengairan*, 1–9.

Dyhouse, G. R. (1985). Stage-Frequency Analysis at a Major River Junction. *Journal of Hydrology Engineering*, 565–583. https://doi.org/10.1061/(ASCE)0733-9429(1985)111:4(565

Erstayudha, N., Hadi, P., & Suprayogi, S. (2016). Model Pemanenan Air Hujan (Rainwater Harvesting) untuk Mengurangi Dampak Bencana Banjir di DAS Penguluran, Kecamatan Sumbermanjing Wetan Kabupaten Malang. *Thesis*, *September*. https://doi.org/10.13140/RG.2.2.21587.58406

Goel, N. K., Than, H., & Arya, D. S. (2005). Flood Hazard Mapping In The Lower Part Of Chindwin River Basin. *International Conference on Innovation Advances and Implementation of Flood Forecasting Technology. Tromsø, Norway.*

Harto B. S. (2000). *Hidrologi: teori, masalah, penyelesaian (Hydrology, theory-problem-solution)*.

Khan, H. U. A., Khalil, S. F. A., Kazmi, S. J. H., Umar, M., Shahzad, A., & Farhan, S. Bin. (2017). Identification of River Bank Erosion and Inundation Hazard Zones Using Geospatial Techniques – a Case Study of Indus River Near Layyah District, Punjab, Pakistan. *Geoplanning: Journal of Geomatics and Planning*, *4*(2), 121. https://doi.org/10.14710/geoplanning.4.2.121-130

Khan, S., Ncibi, K., Hamdi, N., & Hamed, Y. (2022). Flood Analysis Using HEC-RAS and HEC-HMS : A Case Study. *Water*, *14*(3779), 1–19.

Martin, O., Rugumayo, A., & Ovcharovichova, J. (2012). Application of HEC-HMS / RAS and GIS Tools in Flood Modeling : A Case Study for River Sironko –Uganda. *Global Journal of Engineering, Design & Technology*, 19–31.

Pabalik, I., Ihsan, N., & Arsyad, M. (2015). Analisis Fenomena Perubahan Iklim dan Karakteristik Curah Hujan Ekstrim di Kota Makassar. *Jurnal Sains Dan Pendidikan Fisika*, *11*(1), 88–92.

Peraturan Menteri PU RI No12/PRT/M/ 2014. (2014). Peraturan Menteri PU RI No12/PRT/M/ 2014. *Tentang Penyelenggaraan Sistem Drainase Perkotaan*, 1–18.

Rahman, G., Atta-ur-Rahman, Samiullah, & Dawood, M. (2018). Spatial and temporal variation of rainfall and drought in Khyber Pakhtunkhwa Province of Pakistan during 1971–2015. *Arabian Journal of Geosciences*, *11*(3), 46. https://doi.org/10.1007/s12517-018-3396-7

Sachs, L. (1984). *Applied Statistics: A Handbook of Techniques*.

Samarasinghe *et al.* (2010). Application of Remote Sensing and GIS for Flood Risk Analysis: A Case Study at Kalu-Ganga River, Sri Lanka. *International Archives of the Photogrammetry, Remote Sensing and Spatial Information Science, Volume XXXVIII, Part 8, Kyoto Japan*, 110–115.

Santosa, P. B. (2006). River flow prediction and floodplain mapping using Artificial Neural Networks and GIS. *International Symposium & Exhibition on Geoinformation 2006, Malaysia*, 1–7. https://repository.ugm.ac.id/276104/

Shen, X., Li, S., Sun, S., Qing, D., Li, D., Wang, K., Gao, W., & Cao, L. (2023). The mechanism of dissolved oxygen mixing and atmospheric reoxygenation at the confluence with different flow ratios and junction angles. *Journal of Hydrology*, *626*(PA), 130191. https://doi.org/10.1016/j.jhydrol.2023.130191

Soewarno. (1995). *Hidrologi Aplikasi Metode Statistik Untuk Analisa Data*. Penerbit Nova.

Soewarno. (2014). *Aplikasi metode Statistika Untuk Analisis Data Hidrologi.* Graha Ilmu.

Suryanti, I., Nyoman Harry Juliarthana, I., Ayu Sari Galih, K., & Putu Wahyu Wedanta Pucangan, I. (2023). Kajian Topografi dan Hidrologi Sempadan Sungai Tukad Oos Kabupaten Bangli-Gianyar. *Open Access*, *6*(1), 36–49.

Syamsuddin, A. P., Musa, R., & Ashad, H. (2022). Kajian Pengaruh Parameter Hidrograf Satuan Sintetik Berdasarkan Karakteristik Daerah Aliran Sungai. *Jurnal Teknik Sipil MACCA*, *7*(1), 50–56. https://doi.org/10.33096/jtsm.v7i1.541

Tang, X., Li, R., Wu, M., Zhao, W., Zhao, L., Zhou, Y., & Bowes, M. J. (2019). Influence of turbid flood water release on sediment deposition and phosphorus distribution in the bed sediment of the Three Gorges Reservoir, China. *Science of the Total Environment*, *657*, 36–45. https://doi.org/10.1016/j.scitotenv.2018.12.011

Triatmodjo, B. (2008). *Hidrologi terapan (Applied hydrology)*. Beta Offset.

Triatmodjo, B. (2013). *Hidrologi Terapan*. Beta Offset.

Tsakiris, G. (2014). Flood risk assessment: Concepts, modelling, applications. *Natural Hazards and Earth System Sciences*, *14*(5), 1361–1369. https://doi.org/10.5194/nhess-14-1361-2014

Weber, H, P. M. (1988). Possible Contributions of Hydroinformatics to Risk Analysis in Insurance. *Proceedings of the Second International Conference on Hydroinformatics*, 57–62. https://doi.org/ISBN 90 5410 825 5